Acta Crystallographica Section B
Structural Science
ISSN 0108-7681

The phases of $[(CH_3)_4N](ClO_4)$ at low temperature

Elías Palacios,[a]* Ramón Burriel[a] and Paolo Ferloni[b]

[a]Instituto de Ciencia de Materiales de Aragón, CSIC–Universidad de Zaragoza, Facultad de Ciencias, Pedro Cerbuna 12, 50009 Zaragoza, Spain, and [b]Dipartimento di Chimica Fisica and IENI-CNR, Università di Pavia, Viale Taramelli 12, 27100 Pavia, Italy

Correspondence e-mail: elias@posta.unizar.es

Received 1 January 2003
Accepted 28 August 2003

The low-temperature crystal structures of tetramethylammonium perchlorate, $[(CH_3)_4N](ClO_4)$, are analysed. At 210 K, a collection of 376 unique reflections on a single crystal gave $R = 0.0567$ for space group $P4/nmm$, with $a_1 = 8.2376\ (14)$, $c_1 = 5.8256\ (12)$ Å and $Z = 2$, where the ClO_4 groups are disordered over four orientations. Below $T_c = 170$ K, these groups order in four sublattices, each ion gradually choosing one unique orientation. At 150 K, the crystal is microtwinned. 1389 unique reflections were refined in the orthorhombic space group $P2_12_12$, with $a_3 = 11.714\ (3)$, $b_3 = 11.784\ (3)$, $c_3 = 5.8265\ (9)$ Å, $Z = 4$ and $R = 0.087$. At 30 K, Rietveld refinement gave the same structure as is found at 150 K, with a clear difference between a_3 and b_3 [$a_3 = 11.566\ (2)$, $b_3 = 11.806\ (2)$ and $c_3 = 5.729\ (1)$ Å]. The structural models and the phase transition are explained on the basis of electrostatic octopole–octopole interactions among the ClO_4 groups within layers perpendicular to the c axis. The order parameters of the low-temperature phase are discussed in relation to the structural results.

1. Introduction

Tetramethylammonium perchlorate, $[(CH_3)_4N](ClO_4)$, contains tetrahedral tetramethylammonium, $(CH_3)_4N^+$, and perchlorate, ClO_4^-, ions, packed in a structure similar to the CsCl-type but with a lower symmetry; the ClO_4^- ions are orientationally disordered at room temperature (RT). Rotational degrees of freedom produce phase transitions in the similar compound $[(CH_3)_4N](BF_4)$, whose crystal structure (Fig. 1) has been published previously (Giuseppetti *et al.*, 1992; Palacios *et al.*, 1996).

The RT structure of the title compound was reported (McCullough, 1964) as tetragonal ($P4/nmm$ and $Z = 2$, with cell parameters $a_0 = b_0 = 8.343$ and $c_0 = 5.982$ Å); the structure is similar to that of the BF_4 derivative, with B atoms replaced by Cl atoms and F atoms replaced by O atoms. The two structures differ in the positions of the O and F atoms, which define orientations of the ClO_4^- ions that differ from the orientations of the BF_4^- ions. McCullough (1964) reported a poor R value (0.13) in the refinement of 230 reflections measured with Weissenberg and precession cameras. A more recent determination using a four-circle diffractometer (Ilyukhin & Malyarik, 1995) refined 270 unique reflections. Some extra secondary positions for the O atoms were included in the refinement, with smaller occupancy factors. The major positions almost coincide with those of McCullough (1964), but the R value reaches a modest 0.08. In the structure of $[(CH_3)_4N](BF_4)$ (Palacios *et al.*, 1996), it was observed that the positions of the F atoms are not well localized at RT because of the mobility of the BF_4 group for rotations, especially

around the *c* axis, which produces rotational oscillations, called librations, with a high anharmonicity. In the perchlorate compound, these effects are expected to be similar or even enhanced because of the smaller moment of inertia of ClO_4. Most probably it is impossible to obtain a good fit at RT without introducing anharmonicity into the structural model, as happens very often in solids containing small molecular groups loosely linked to the remaining atoms in the crystal (Vogt & Prandl, 1983).

Therefore, it is advisable to study the structure at low temperature (LT), at which the smaller thermal motion allows a better localization of the atoms. The calorimetric study of $[(CH_3)_4N](BF_4)$ revealed two phase transitions at 158 and 612 K, which are due to successive steps of orientational disordering of the BF_4 groups *via* electrostatic octopole–octopole interactions. In $[(CH_3)_4N](ClO_4)$, the Cl—O distance is similar to the B—F distance, and the O-atom charge is probably similar to that of the F atom, so the behaviour of the two compounds is expected to be similar. Actually, the heat capacity of $[(CH_3)_4N](ClO_4)$ (Burriel *et al.*, 2002) has two sharp peaks at $T_c = 169.8$ and 614 K, which are attributable to phase transitions connected to these disordering processes. We study here the crystal structure of the LT phases of $[(CH_3)_4N](ClO_4)$ by X-ray diffraction.

2. Experimental

Single crystals were grown at RT by recrystallization from aqueous solutions of Fluka purum $[(CH_3)_4N](ClO_4)$. X-ray diffraction measurements on single crystals were carried out with a four-circle Siemens diffractometer using Mo $K\alpha$ radiation and a point detector. For the cryogenic system, an Oxford Instruments cold-nitrogen-jet device was used. The temperature was checked by replacing the crystal with a thermocouple that maintained the same conditions of gas flow and temperature control. It was found that the experimental temperatures were ~150 (5) and 210 (5) K for two LT intensity collections. The linear absorption coefficient is $\mu = 0.45\ mm^{-1}$ ($\mu r \simeq 0.05$), and therefore no absorption correction was made.

Complementarily, powder diffraction patterns on ground single crystals were recorded from RT down to 30 K. This kind of experiment does not have the same precision in intensity as a single-crystal diffraction experiment, but keeps a better temperature control, allows lower working temperatures and avoids problems related to twinning of the crystal in the LT phase. A rotating anode device source, operating at 45 kV and 80 mA, was used with Cu $K\alpha$ radiation ($\lambda_1 = 1.54056$ and $\lambda_2 = 1.54443$ Å), a graphite monochromator and a D-max Rigaku diffractometer. For measurements in the temperature range 30–200 K, an Oxford Instruments helium flow device was used. The sample was held on an aluminium plate, the temperature of which was measured by means of a thermocouple attached to the sample holder. The correspondence of this temperature to that of the sample was checked by comparing the appearance of superstructure reflections in the present sample and in other salts previously studied, such as NH_4MgF_3 and $(NH_4)_2MgF_4$, which undergo well defined first-order transitions at 107.5 (1) and 163.0 (5) K, respectively (Subías *et al.*, 1996). Thus, the temperature settings can be considered accurate within 1 K. The data were analysed with the *FULLPROF*3.5 computer program (Rodríguez-Carvajal *et al.*, 1987).

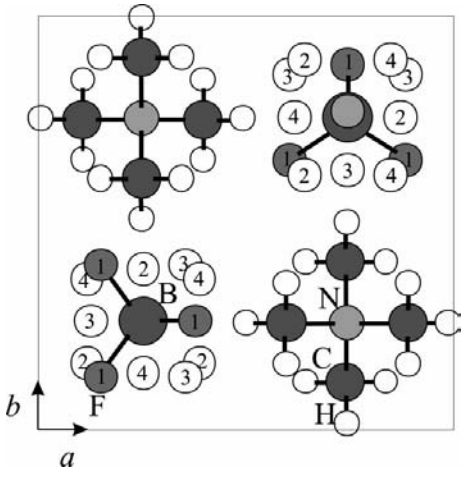

Figure 1
Projection of the 200 K structure of $[(CH_3)_4N](BF_4)$ (Palacios *et al.*, 1996) along the *c* axis. $[(CH_3)_4N](ClO_4)$ has the same type of structure at 210 K, if we replace F atoms by O atoms and B atoms by Cl atoms. The ClO_4^- or BF_4^- ions are randomly disordered over four orientations (numbered 1 to 4 in the text). The F or O atoms corresponding to the orientation of each sublattice are marked with the same number. The low-temperature ordering mode is represented by grey circles.

3. Results and data analysis

3.1. Single-crystal data

3.1.1. 210 K. The reflections could be indexed in the tetragonal space group *P*4/*nmm*. Experimental details are listed in Table 1.[1] The reported cell parameters were derived from the powder diffraction pattern because of the better precision in temperature for this kind of experiment. For the positions of the N, Cl and C atoms, the structures described by McCullough (1964) and Palacios *et al.* (1996) were taken as a starting point. Data were analysed with *SHELXL*97 (Sheldrick, 1997). Fourier difference synthesis revealed the positions of the H atoms and one O atom, labelled O1 throughout this paper. There were no peaks that could be easily identified with the remaining O atoms in a physically rational way (Fig. 2), which indicates that the O atoms are distributed in a wide region of space, whereas the much lighter H atoms give clear Fourier peaks. The Cl—O and O—O distances were restrained to be equal within 0.003 Å. The final fitting parameters are shown in Table 2 and in the supplementary material.[1] Performing a standard free refinement gives a slightly better fit, with large standard deviations for the positions of the O atoms. Moreover, the *x* coordinates for atoms O1 and Cl

[1] Supplementary data for this paper are available from the IUCr electronic archives (Reference: BS0018). Services for accessing these data are described at the back of the journal.

Table 1
Experimental details.

	Single crystal, 210 K	Single crystal, 150 K	Powder, 100 K	Powder, 30 K
Crystal data				
Chemical formula	$C_4H_{12}N{\cdot}ClO_4$	$C_4H_{12}N{\cdot}ClO_4$	$C_4H_{12}N{\cdot}ClO_4$	$C_4H_{12}N{\cdot}ClO_4$
M_r	173.60	173.60	173.60	173.60
Cell setting, space group	Tetragonal, *P*4/*nmm*	Orthorhombic, $P2_12_12$	Orthorhombic, $P2_12_12$	Orthorhombic, $P2_12_12$
a, *b*, *c* (Å)	8.2376 (14), 8.2376 (14), 5.8256 (12)	11.714 (3), 11.784 (3), 5.8265 (9)	11.639 (3), 11.798 (3), 5.7790 (13)	11.566 (2), 11.806 (2), 5.7292 (11)
V (Å^3)	395.31 (13)	804.3 (3)	793.6 (3)	782.3 (3)
Z	2	4	4	4
D_x (Mg m^{-3})	1.458	1.434	1.453 (4)	1.474 (4)
Radiation type	Mo $K\alpha$	Mo $K\alpha$	Cu $K\alpha$	Cu $K\alpha$
No. of reflections for cell parameters	45	55	–	–
θ range (°)	3.5–30.4	1.7–30.1	–	–
μ (mm^{-1})	0.45	0.44	–	–
Temperature (K)	210 (1)	150 (1)	100 (1)	30 (1)
Specimen form, colour	Prism, colourless	Prism, colourless	Flat sheet (particle morphology: irregular), white	Flat sheet (particle morphology: irregular), white
Specimen size (mm)	0.3 × 0.2 × 0.2	0.3 × 0.2 × 0.2	20 × 10 × 1	20 × 10 × 1
Data collection				
Diffractometer	Siemens *P*4	Siemens *P*4	D-max Rigaku	D-max Rigaku
Data collection method	ω–2θ scans	ω–2θ scans	Mode: reflection; scan method: step	Mode: reflection; scan method: step
No. of measured, independent and observed reflections	1534, 376, 331	1729, 1389, 1210	–	–
Criterion for observed reflections	$I > 2\sigma(I)$	$I > 2\sigma(I)$	–	–
R_{int}	0.046	0.027	–	–
θ_{max} (°)	30.5	30.1	$2\theta_{min}$ = 5, $2\theta_{max}$ = 60, increment = 0.03	$2\theta_{min}$ = 5, $2\theta_{max}$ = 60, increment = 0.03
Range of *h*, *k*, *l*	$-1 \Rightarrow h \Rightarrow 11$ $-1 \Rightarrow k \Rightarrow 11$ $-8 \Rightarrow l \Rightarrow 8$	$-1 \Rightarrow h \Rightarrow 16$ $-1 \Rightarrow k \Rightarrow 16$ $-8 \Rightarrow l \Rightarrow 4$	– – –	– – –
No. and frequency of standard reflections	3 every 60 min	3 every 60 min	–	–
Refinement				
Refinement on	F^2	F^2	I_{net}	I_{net}
$R[F^2 > 2\sigma(F^2)]$, $wR(F^2)$, S	0.057, 0.136, 1.25	0.087, 0.248, 1.88	R_p = 0.130, R_{wp} = 0.179, R_{exp} = 0.128, S = 1.40	R_p = 0.139, R_{wp} = 0.189, R_{exp} = 0.127, S = 1.49
Reflection/profile data	376 reflections	1389 reflections	Wavelength of incident radiation = 1.540562–1.544390 Å; excluded region(s): none; profile function: pseudo-Voigt	Wavelength of incident radiation = 1.540562–1.544390 Å; excluded region(s): none; profile function: pseudo-Voigt
No. of parameters	36	99	34	34
H-atom treatment	Mixture of independent and constrained refinement	Mixture of independent and constrained refinement	Not refined	Not refined
Weighting scheme	$w = 1/[\sigma^2(F_o^2) + (0.043P)^2 + 0.1615P]$ where $P = (F_o^2 + 2F_c^2)/3$	$w = 1/[\sigma^2(F_o^2) + (0.1P)^2]$ where $P = (F_o^2 + 2F_c^2)/3$	$w = 1/y$	$w = 1/y$
$(\Delta/\sigma)_{max}$	<0.0001	0.049	0.02	0.02
$\Delta\rho_{max}$, $\Delta\rho_{min}$ (e Å^{-3})	0.73, −0.66	1.27, −1.39	–	–

Computer programs: *XSCANS* (Siemens, 1990), *IUSA* (Rigaku Corporation, 1992), *FULLPROF*3.5 (Rodriguez-Carvajal *et al.*, 1987), *SHELXL*97 (Sheldrick, 1997).

(which lie very near to the fourfold axis) have to be fixed. From the position of atoms O2 and O3 and the tetrahedral shape of the ClO_4 group, we can derive $x(O1) = 0.274$ and $x(Cl) = 0.230$, with $R = 0.048$.

The structural model proposed in this work gives a substantially better fit ($R = 0.057$) than the model reported by McCullough (1964) applied to our experimental data [$R = 0.089$ for the 331 observed unique reflections, which is similar to the value obtained by Ilyukhin & Malyarik (1995)], but in such a critical case this numerical difference may not be significant. Therefore, some physical considerations will be added. The fourfold axis close to the Cl—O1 direction requires that the ClO_4 group must be disordered over at least four orientations. Because of the tetrahedral shape of the ion, the remaining O atoms must be distributed in at least 12 positions, near a circle of radius $d8^{1/2}/3 = 1.34$ Å, where d is

Table 2
Site symmetries, multiplicities, Wyckoff symbols, atomic coordinates and equivalent isotropic displacement parameters (Å^2) for $(CH_3)_4NClO_4$ at 210 K.

The Cl—O and O—O distances have been restrained to be equal, within 0.003 Å, in order to preserve the tetrahedral shape of the ClO_4 group. U_{eq} is defined as one third of the trace of the U^{ij} tensor.

	Symmetry	Wyckoff position	x	y	z	U_{eq}
N	$\bar{4}m2$	2(b)	3/4	1/4	1/2	0.025 (1)
C	.m.	8(i)	1/4	0.6030 (3)	0.3538 (4)	0.041 (1)
Cl	.m.	8(i)	0.2307 (8)	1/4	−0.0742 (2)	0.025 (1)
O1	4mm	2(c)	1/4	1/4	0.1644 (6)	0.053 (1)
O2	1	16(k)	0.1453 (11)	0.3892 (5)	−0.1398 (7)	0.069 (3)
O3	.m.	8(i)	0.3832 (12)	1/4	−0.1790 (11)	0.143 (10)

the Cl—O distance. The average distance between the 12 positions is only ∼0.75 Å, similar to the r.m.s. amplitude of the thermal motion, which explains both the absence of sharp peaks in the Fourier plot and the large anharmonicity of the librational motion.

The $P4/nmm$ group has two non-equivalent mirror planes intersecting at each fourfold axis and making an angle of 45° with one another. In combination with the fourfold symmetry, the condition of having only four minimum energy orientations means that one of these planes must coincide with a mirror plane of the tetrahedral ClO_4^- ion: that is, atoms Cl, O1 and O3 must lie in such a plane. One possibility (Figs. 1 and 2) is that this is the mirror plane containing atom O3 and passing through the nearest N atoms (.m. plane). An alternative option, chosen by McCullough (1964) and Ilyukhin & Malyarik (1995), is the plane passing through the nearest ClO_4^- ions (..m plane). Other possibilities would require more than four equivalent orientations, which is physically unlikely and does not agree with the heat capacity data; the anomalous molar entropy of the transition at 170 K is $\Delta S/R = \ln 4$ (Burriel *et al.*, 2002), which implies only four orientations. Only the question of which mirror plane is occupied by atom O3 remains to be solved. Fig. 2 shows a section of the observed Fourier synthesis at $z/c = 0.83$, a plane passing near the centres of atoms O2 and O3. Indeed, there is only one non-equivalent maximum, at (0.35, 0.15, 0.83), but this can be explained as being formed by two peaks (at a distance of 0.4 Å) produced by equivalent O atoms (both labelled O2) in the average disordered structure. The position of atom O3 is in a zone with relatively lower electron density, while the proximity of the two O2 atom peaks results in a higher density. If the maximum of the double peak were identified with atom O3 [the option chosen by McCullough (1964)], the tetrahedral geometry of the ClO_4^- ion together with the fourfold symmetry axis would lead to the occurrence of the two O2 atoms in the zone where the electron density is relatively lower (*i.e.* the atomic locations of Fig. 2 would be turned through 45°), which is hardly acceptable.

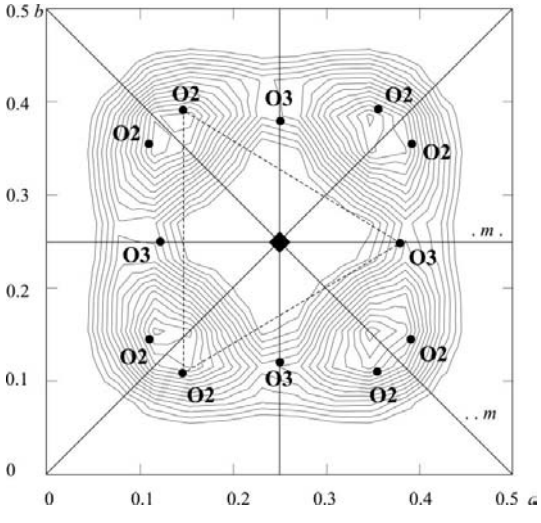

Figure 2
Fourier difference synthesis section, when atoms O2 and O3 are omitted, taken on the plane $z = 0.83$, passing near the centres of these atoms. The dashed triangle joins the atomic positions belonging to the same orientation of the ClO_4^- ion. The projection of the $P4/nmm$ mirror planes .m. and ..m along the c axis are represented by continuous lines. The central filled square represents the projection of the fourfold axis.

The displacement parameters indicate an average r.m.s. motion of ∼0.25 Å, which is of the same order of magnitude as the distance between two minima. McCullough (1964) also gives similar thermal motion amplitudes. Therefore, the present analysis indicates that the ClO_4 group experiences rotational jumps around the fourfold axis among the equivalent orientations. The large value of $U_{11} = U_{22}$ for atom O1 (about twice the value of U_{33}) indicates that this group undergoes large packing librations about this axis; the Cl atom remains more localized than the O atoms.

The potential energy of the ClO_4 group has been calculated as a function of the orientation, assuming the atoms to be point charges. The resulting potential has a wide minimum for rocking oscillations of the Cl—O1 bond and is quasi-isotropic with respect to ion rotations around this bond. Of course, in the real system, there are also short-range intermolecular forces, but the effective potential allows fast rotational jumps at temperatures as low as 210 K, which explains the relatively large displacement parameters for the O atoms compared with those of the N and C atoms. The Raman and IR spectra (Mylrajan & Srinivasan, 1991) show low-frequency bands near 100 cm^{-1}, which correspond to librations and are consistent with the large r.m.s. displacement amplitudes.

3.1.2. 150 K. In a first analysis, the diffractometer automatic indexing procedure gave tetragonal symmetry, $P\bar{4}2_1m$, with cell parameters $a_2 = b_2 = 11.768$ (6) and $c_2 = 5.814$ (3) Å, *i.e.* similar to the BF_4 compound (Palacios *et al.*, 1996). The structure was then refined using the same procedures, and the same structure was found as for the low-temperature phase of $[(CH_3)_4N](BF_4)$, with a poor R value (0.095). This approximate structure is depicted in Fig. 3 and will be cited in the discussion.

However, the profile of the peaks widens across the transition and the internal consistency index for equivalent reflections is as poor as 0.11, whereas for the Friedel pairs it is 0.027; this result gives an idea of the experimental error in the measurement of the intensities. In addition, the powder

diffraction pattern at 30 K clearly reveals an orthorhombic distortion (see below). Since the heat capacity measurements taken between 30 and 150 K did not detect any phase transition, we can assume that the symmetry at 150 K should be retained down to lower temperatures. There is therefore a contradiction between the powder and the single-crystal data that should be explained. On the basis of the systematic absences, and taking into account the space group found at 30 K for the powder sample, the orthorhombic group $P2_12_12$ was chosen to index the structure of the compound at 150 K. Experimental details are gived in Table 1. In this structural model, the ClO_4 group is slightly rotated around an axis perpendicular to the picture, with respect to the orientation shown in Fig. 3.

A third possibility was also checked. The final Rietveld refinement on powder data at 30 K (see below) gave a structure near to the centrosymmetric *Pbma*, which would be reached if atoms O1, O2 and Cl were in a plane perpendicular to *b* at $y = \frac{1}{4}$ (the *.m.* plane of the space group), with small displacements of the remaining atoms. For the single crystal, the systematic absences could be undetectable as a result of twinning (*i.e.* the 0*kl* reflections with $k = 2n + 1$ and the *hk*0 reflections with $h = 2n + 1$ are forbidden for one individual but allowed for the other). Some exceptions are the *hk*0 reflections with odd *h* and *k*, which are forbidden for both individuals by the *Pbma* group. There are some weak but observed reflections of this kind, such as $1\bar{1}0$, 310 and $3\bar{1}0$ with $15 > I/\sigma(I) > 5$. Moreover, this structure type cannot be reached continuously from that found at 210 K in a second- or weak first-order transition, such as the transition found in heat capacity measurements. In any case, the experimental data were also analysed using the *Pbma* group, which gave $R = 0.098$, an even worse result than that for the tetragonal group $P\bar{4}2_1m$. Thus, the non-centrosymmetric group $P2_12_12$ was maintained.

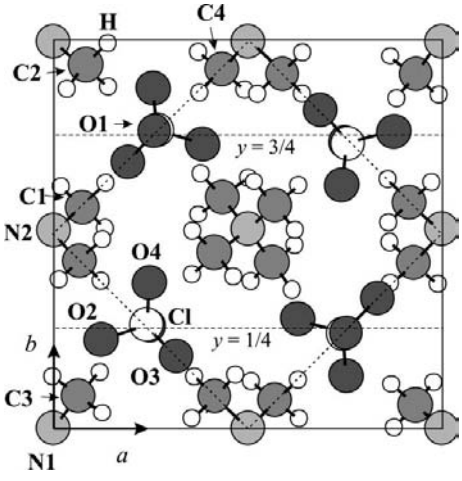

Figure 3
Projection of the 150 K approximate structure of $[(CH_3)_4N](ClO_4)$ along the *c* axis, analysed as tetragonal, with space group $P\bar{4}2_1m$. The slanted dashed lines show mirror planes that would force the O3 atoms to remain in this plane if the structure exactly matched this model. The horizontal dashed lines represent the mirror planes at $y = \frac{1}{4}$ and $\frac{3}{4}$ of the other possible pseudosymmetry, *Pbma*.

Table 3
Site symmetries, Wyckoff multiplicities, atomic coordinates and equivalent isotropic displacement parameters (Å^2) for $(CH_3)_4NClO_4$ at 150 K.

U_{eq} is defined as one third of the trace of the orthogonalized U^{ij} tensor.

	Symmetry	Wyckoff position	*x*	*y*	*z*	U_{eq}
Cl	1	4(*c*)	0.2403 (1)	0.2557 (2)	0.0709 (2)	0.027 (1)
O1	1	4(*c*)	0.2506 (3)	0.2516 (5)	−0.1730 (4)	0.037 (1)
O2	1	4(*c*)	0.1234 (3)	0.2409 (6)	0.1334 (7)	0.057 (1)
O3	1	4(*c*)	0.3070 (7)	0.1673 (8)	0.1702 (8)	0.144 (6)
O4	1	4(*c*)	0.2795 (7)	0.3629 (6)	0.1522 (12)	0.099 (4)
N1	..2	2(*a*)	0	0	0.4969 (17)	0.027 (2)
N2	..2	2(*b*)	0	1/2	0.4873 (11)	0.023 (2)
C1	1	4(*c*)	0.0740 (7)	0.5699 (10)	0.3321 (17)	0.040 (2)
C2	1	4(*c*)	0.0833 (5)	−0.0646 (8)	0.3554 (16)	0.029 (2)
C3	1	4(*c*)	0.0646 (6)	0.0834 (8)	0.6448 (17)	0.030 (2)
C4	1	4(*c*)	0.0719 (7)	0.4254 (9)	0.6384 (17)	0.038 (2)

Two kinds of microtwins appear in passing from the tetragonal $P\bar{4}2_1m$ to the orthorhombic $P2_12_12$ group, and this phenomenon is assumed to be the cause of the widening of peaks on the occurrence of the phase transition. The fitted parameters were the atomic coordinates and displacement parameters and the volume fractions of the twin components. The existence of a predominant kind of twin [occupation 0.745 (9)] allows the localization of the H atoms by Fourier difference. The refinement of their positions gave results very close to those assumed *a priori*. The final set of refined parameters assuming a single orientation for the ClO_4 group on each site are given in Table 3 and the supplementary material. Because of the symmetry requirements, the orientation on one site defines the orientation on the other sites according to the pattern shown in Fig. 3. The final Fourier difference synthesis gave some peaks (the most intense peak and hole are 1.27 and −1.39 e Å^3 high, respectively), which are probably due either to some degree of remaining disorder at a temperature not far below T_c or to imprecise measurement of the intensities in a microtwinned orthorhombic crystal.

In another analysis, refinable occupation numbers for different ClO_4 orientations were fitted. In order to reduce the number of refinable parameters, isotropic displacement parameters were used. An interesting feature is that in the final stage of refinement only two of the four possible orientations of the ClO_4^- ion at each site are really present, the majority of these ions (85%) being aligned in one orientation and the remainder (15%) being turned 90° around the *c* axis.

3.2. Powder diffraction data

3.2.1. 30 K. The indexing procedure was performed as described by Subías *et al.* (1996), based on the assumption that, when a second-order or a weak first-order transition occurs, the substructure reflections split or change their position in the pattern, but their intensities do not change dramatically. By varying the unit-cell parameters while fixing the intensities and widths of the peaks (taken from the phase above T_c), it was possible to match all the substructure intensities with an orthorhombic unit cell. On the basis of the superstructure reflections observed, the diffractogram (Fig. 4)

could be indexed in space group $P2_12_12$, which can be obtained from the RT cell by the transformation $\mathbf{a}_3 = \mathbf{a}_1 + \mathbf{b}_1$, $\mathbf{b}_3 = -\mathbf{a}_1 + \mathbf{b}_1$ and $\mathbf{c}_3 = \mathbf{c}_1$ plus a general thermal contraction and a small orthorhombic distortion making $a_3 \neq b_3$. At 30 K, some multiple reflections, such as 040 + 400 ($2\theta = 30.24$ and 30.89°) or 241 + 421 ($2\theta = 37.60$ and 38.00°), are very clearly split, whereas some others, *hhl*, such as 221 or 331, remain single, excluding a monoclinic distortion. The N, C, Cl and H atoms were placed in positions obtained from the structure at 150 K. Two data analyses were made. In the first, the positions of the O atoms were found from a difference Fourier map, which for powder diffraction is a less reliable procedure than it is for single-crystal data. In the second analysis, the O atoms were refined from their positions at 150 K. In each case, the final positions converged to the same coordinates and had better localization than at 150 K, but the $(CH_3)_4N^+$ and ClO_4^- ions were quite substantially distorted from tetrahedral geometry. In the final refinement stage, rigid-group constraints were applied in order to reduce the number of fitting parameters. For the ClO_4^- ion, the refinable parameters were the position of the Cl atom, the Euler angles, the Cl—O distance and one isotropic displacement parameter for each kind of atom. For each of the two non-equivalent $(CH_3)_4N$ groups, the refined parameters were the position, the Euler angle, φ, the N—C distance and the two independent C—N—C angles. The final C—N—C angles range from 103.8 (4) to 110.7 (4)°. The displacement parameters for the N and C atoms became slightly negative (very probably because of the transparency of the sample) and were fixed to zero. The H atoms were introduced in tetrahedral positions, with C—H distances of 1 Å. The most significant structural fitting parameters are given in the supplentary material (see also Table 4), and the observed, calculated and difference patterns are shown in Fig. 4. The projection of the structure along the *c* axis is illustrated in Fig. 5.

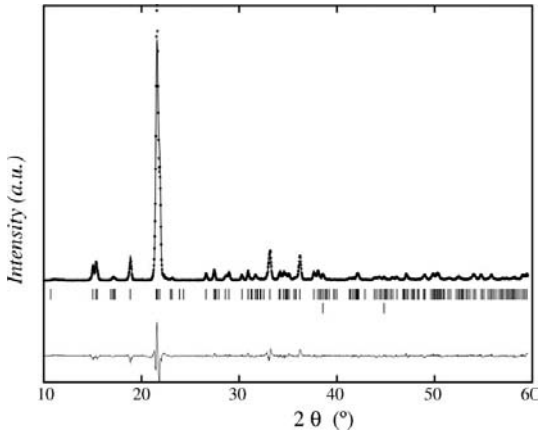

Figure 4
Rietveld refinement at 30 K, showing the observed (circles), calculated and difference patterns (continuous lines). The ticks indicate the positions of the Bragg reflections for Cu $K\alpha_1$ and Cu $K\alpha_2$ radiation and the cell parameters given in Table 1. The 111 and 200 reflections of Al, which originate from the sample holder, have also been included in the refinement and are each identified as a pair of ticks at $2\theta = 38.5$ and 44.8°.

Table 4
Refined Euler angles (φ, θ, ψ).

The orientation (0,0,0) corresponds to the situation described in Fig. 3.

	φ (°)	θ (°)	ψ (°)
ClO_4	−3.02 (13)	−6.58 (1)	6.48 (4)
$N1(CH_3)_4$	6.99 (2)	0	0
$N2(CH_3)_4$	−5.75 (2)	0	0

As noted above, the atomic positions are close to conforming to the symmetry operations of space group *Pbma*. The different systematic absences for the two groups are not clearly distinguishable. Analysis of the pattern with *Pbma* gives a good refinement, with fewer free parameters than the refinements in $P2_12_12$, and could be experimentally satisfactory. The interatomic distances and angles for the tetramethylammonium ion have values closer to those obtained in the single-crystal diffraction study at 210 K [N—C = 1.480 (2) Å]. From the analysis of the patterns at several temperatures below T_c it can be concluded that there is a gradual rotation of the ClO_4 group, in which the structure changes from near tetragonal to close to the centrosymmetric *Pbma*. As discussed for the crystal at 150 K, the non-centrosymmetric $P2_12_12$ group was chosen.

3.2.2. 100 K. The structure is the same as that found at 30 K, $P2_12_12$, with $a = 11.639$ (3), $b = 11.798$ (3), $c = 5.7790$ (14) Å and $Z = 4$, giving a Bragg reliability index of $R_B = 0.062$. The strain or relative difference $(b - a)/a = 0.014$ is considerably lower than the value of 0.021 obtained at 30 K. The positions of the O atoms approach the 'ideal' positions in a tetragonal structure as described at 150 K, and indeed the pattern fits slightly better with the $P2_12_12$ group than with *Pbma*. The occupation factors for atoms O2, O3 and O4 were refined but are close to 1. There are no significant changes in the positions of the remaining atoms.

3.2.3. 200 K. The observed, calculated and difference patterns are shown in Fig. 6. As usual, the refined data are the

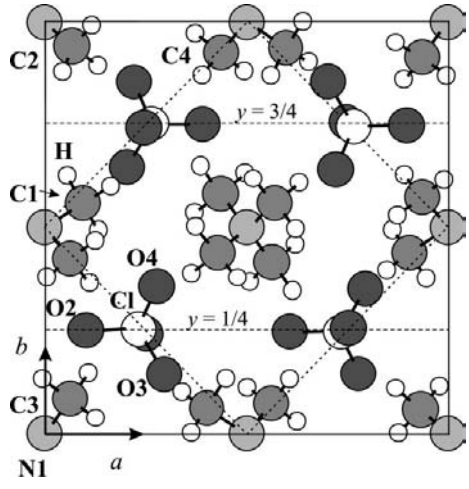

Figure 5
Projection of the structure of $[(CH_3)_4N](ClO_4)$ at 30 K along the *c* axis. The equilibrium orientation of the ClO_4^- ions rotates gradually, bringing atom O3 away from the plane of the N atoms (dashed), which would be a mirror plane for the tetragonal $P\bar{4}2_1m$ space group.

profile values, but the diffraction peaks do not overlap and the quality of the fit is mainly shown by the Bragg index. The structure is the same as that found for the single crystal at 210 K, $P4/nmm$, with $a = 8.2369\ (14)$, $c = 5.8251\ (12)$ Å, $Z = 2$ and $R_B = 0.044$. The atomic displacement parameters are all very large, especially those of the O atoms, which are so large that these atoms cannot be considered as localized in any way.

3.2.4. Scan in temperature. In addition to the patterns mentioned in the previous sections, a series of short diffractograms were taken at temperatures between 100 and 180 K, in the range $14 < 2\theta < 40^\circ$, with the aim of studying the thermal evolution of the orthorhombic distortion. Some of these are shown in Fig. 7. The gradual ordering of the ClO_4 groups on cooling is reflected in the appearance and growth of some superstructure reflections (hkl, with $h + k = 2n + 1$ referred to the orthorhombic unit cell), which reflect the doubling of the unit-cell volume of the $P4/nmm$ structure. The most intense reflections, which can be observed below 170 K, are 230, 231 and 210, indexed with respect to the orthorhombic cell. The intensities obtained by integration of the peaks are shown in Fig. 8 as functions of temperature. The substructure reflection 111 is also shown as a reference, since it is far enough from the other reflections and remains single across the transition. The increase of the difference $b - a$ can also be deduced from the splitting of the peaks hkl, with $h \neq k$, below T_c, especially when h is very different from k, such as the reflections 400 and 040 (Fig. 7). Nevertheless, this splitting is hardly observable above 160 K. The cell parameters were fitted for each pattern with the profile parameters fixed to their values at 100 K and the structural parameters fixed to the values found at 150 K for the single crystal. The strain $(b - a)/a$ is shown in Fig. 8 as a function of temperature.

4. Discussion

A set of four parameters, named p_1, p_2, p_3 and p_4, are introduced to describe the possibility of orientational disorder for the ClO_4 group. With p_1, we indicate the majority occupation factor for atoms O2, O3 and O4 in the corresponding position of the LT structure, labelled 1 in Fig. 1. The order parameters p_2, p_3 and p_4 are the occupation factors for O-atom positions corresponding to a ClO_4 group rotated by 90, 180 and 270°, respectively, around the fourfold axis of the disordered structure. The O-atom positions corresponding to these ion orientations are labelled 2, 3 and 4 in Fig. 1. Moreover, the condition $p_1 + p_2 + p_3 + p_4 = 1$ is imposed, so that at very low temperature $p_1 \simeq 1$ and above T_c the structure is fully disordered, with $p_1 = p_2 = p_3 = p_4 = \frac{1}{4}$.

As suggested in §1, the packing of the $(CH_3)_4N^+$ and ClO_4^- ions is quite similar to that of CsCl. Considering layers of unit cells perpendicular to the c axis, the distance between nearest cations or anions is similar within a layer and between layers. Nevertheless, considering all atoms as point charges, the

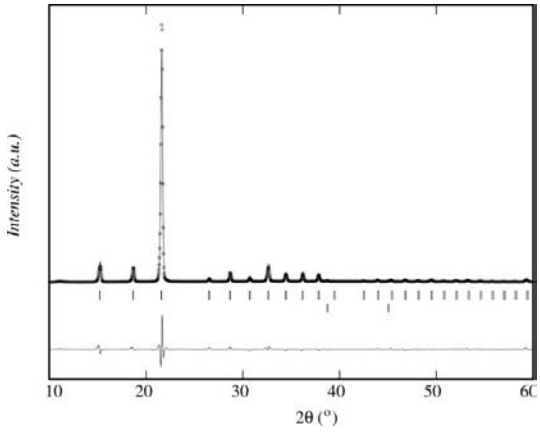

Figure 6
Rietveld refinement at 200 K, showing the observed, calculated and difference patterns. Symbols are the same as in Fig. 4.

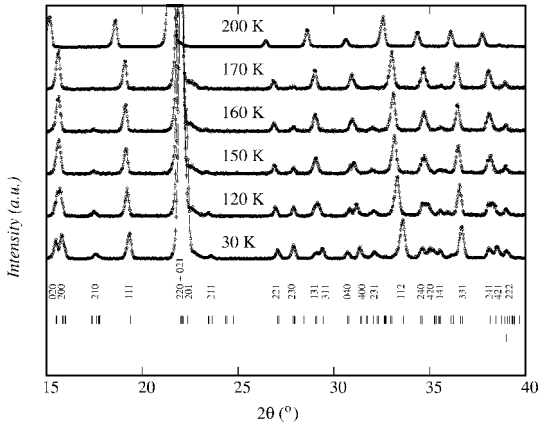

Figure 7
Powder patterns taken at several temperatures. The indices of the most representative Bragg reflections with respect to the orthorhombic $P2_12_12$ cell are reported. Some peaks split below 150 K, thus indicating the orthorhombic distortion. The splitting of the pairs 400 + 040 or 240 + 420 is especially remarkable. The superstructure reflections ($h + k = 2n + 1$), such as 230 or 141, are already observed at 170 K, where the orthorhombic distortion is not yet noticeable.

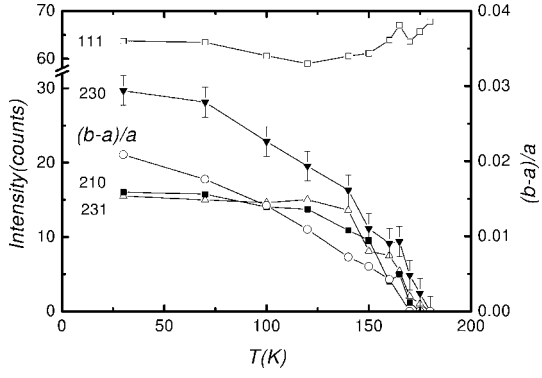

Figure 8
Strain, $(b - a)/a$ (right scale), and intensity (left scale) of some superstructure reflections as functions of temperature for the LT phase. The error bars on intensities are similar for all the reflections but are depicted only for the 230 reflection for clarity. The error bars on strain are smaller than the symbol. The substructure reflection 111 is shown as a reference.

electrostatic interaction between two ClO_4^- ions shows that the interaction energy is virtually independent of the relative orientation of the ions in different layers. In any case, when each layer orders, even the weakest interlayer interaction would produce the ordering of the entire lattice. The anomalous heat capacities of $[(CH_3)_4N](ClO_4)$ and $[(CH_3)_4N](BF_4)$ suggest an interlayer interaction ~20% as large as the intralayer one (Burriel *et al.*, 2002). This interaction has to be directed *via* the electronic or molecular polarization of the $(CH_3)_4N^+$ ions. The electrostatic intermolecular interaction was computed for $[(CH_3)_4N](BF_4)$, considering the nearest neighbours in a layer for all the different relative orientations. In an ordered domain, a 90 or 270° rotation of a single ion requires an energy of $E/k_B = 510$ K ($k_B = 1.381 \times 10^{-23}$ J K^{-1} is the Boltzmann constant), which is about half the energy required for a 180° rotation (Palacios *et al.*, 1996, Fig. 7 and Table V). Since the similar interatomic distances and transition temperatures indicate a similar octopole moment, these calculations also seem applicable to $[(CH_3)_4N](ClO_4)$. Therefore, slightly below T_c, a partially ordered structure can be expected, with $p_1 > p_2 = p_4 > p_3$. The observed case at 150 K is $p_1 = 0.85$, $p_2 = 0.15$ and $p_3 = p_4 = 0$, but experimentally both situations give the same superstructure reflections. The two situations are only distinguished by a small difference in the substructure reflections, and calculating the intensities for both possibilities, it becomes clear that the difference is smaller than the experimental error. Therefore, from the experimental data, $p_1 > p_2 = p_4 > p_3$ can be assumed.

This possibility is also predicted by Monte Carlo simulations, as can be observed in the analogous BF_4 derivative (Palacios *et al.*, 1996, Fig. 11). Slightly below T_c, there are four kinds of domain, namely the majority domain (type 1), two less populated domains (types 2 and 4), with orientations turned 90 and 270° with respect to type 1, and the least populated domain (type 3), which corresponds to rotations of 180° with respect to type 1. At T_c, all four domains are equally probable, but a domain wall between type 3 and type 1 requires more energy than between types 2 or 4 and type 1. Therefore, when some fluctuation causes the type 1 domain to become dominant, the population of type 3 becomes smaller than that of types 2 or 4. At low temperatures, there are some isolated type 2 and 4 small domains in the 'sea' of type 1 but almost none of type 3.

In the phase above T_c, the point group at the site of the ClO_4^- ion is 4*mm* (C_{4v}). Consider four sublattices such that the state of each ClO_4^- ion can be obtained by the application of the symmetry operations of the $P2_12_12$ group, as observed experimentally and also predicted by Monte Carlo simulations: that is, let us assume that in the fully ordered state, when a ClO_4^- ion has a given orientation, the nearest anions are obtained as shown in Figs. 1 and 3, in which their orientations are symmetrically equivalent, uniquely defined and labelled as 1 in Fig. 1. The other possible orientations, 2, 3 and 4, are obtained from 1 by successive 90° counterclockwise rotations of the lower-left ion and the corresponding sense for the rest. In a partially disordered state, the ClO_4^- ion jumps between orientations in such a way that several orientations have a non-zero occupation probability, p_i. We will assume that these probabilities are the same for every ClO_4^- ion. If not, the symmetry cannot be described as $P2_12_12$ with the lattice constants given.

For the sake of simplicity, and as a first approximation, we will also assume that, below T_c, atom O3 remains in the plane containing the nearest N atoms (*i.e.* the *..m* plane of $P\bar{4}2_1m$, which is approached just below T_c), although it has been shown experimentally that atom O3 departs markedly from this position at very low temperatures. The symmetry-adapted order parameters are defined as

(i) $q_0 = p_1 + p_2 + p_3 + p_4$, which transforms according to the symmetric representation A_1 of the point group 4*mm* (C_{4v}) and always equals 1;

(ii) $q_1 = p_1 - p_2 + p_3 - p_4$, which transforms according to the representation B_1;

(iii) the pair $q_2 = p_1 + p_2 - p_3 - p_4$ and $q_3 = p_1 - p_2 - p_3 + p_4$, which transform according to the two-dimensional representation E.

Above T_c, all orientations are randomly occupied; the only non-zero parameter is q_0 and the structure is tetragonal, as the occupation is fully symmetric with respect to the 4*mm* group. At low temperature, at least another q_i has to be non-zero. According to Landau theory (Tolédano & Tolédano, 1987), one kind of order is associated with each irreducible representation. A phase transition is possible if the second-order coefficient in the free-energy expansion decreases on cooling and eventually becomes negative below some critical temperature. There could be several transitions between different phases characterized by the parameters q_i that differ from zero. However, when the critical temperatures for two representations are not very different, the higher-order coupling terms between the order parameters usually cause the transitions to collapse together in a second- or a weak first-order transition. The occurrence of this collapse depends on the sign and relative values of the fourth-order coefficients in the Landau free-energy expansion.

Another implication of the Landau theory is that one of the parameters corresponding to the same representation q_2 or q_3 is zero, or that $|q_2| = |q_3|$. Assuming the occupation p_1 to be the highest, let us analyse the different possibilities:

(*a*) The case $q_1 = 0$, $q_2 > 0$ and $q_3 = 0$ corresponds to $p_1 = p_2 > p_3 = p_4$, or equivalently $q_1 = 0$, $q_2 = 0$ and $q_3 > 0$, which gives $p_1 = p_4 > p_2 = p_3$.

(*b*) The case $q_1 = 0$ and $q_2 = q_3 > 0$ corresponds to $p_1 > p_3$ and $p_2 = p_4 = \frac{1}{4}$, and is equivalent to the cases $q_2 = -q_3$ (the majority now being p_2 or p_4, depending on the sign of q_2) or $q_2 = q_3 < 0$, which gives p_3 as the majority.

(*c*) The case $q_1 > 0$ and $q_2 = q_3 = 0$ implies $p_1 = p_3 > p_2 = p_4$. Complete order would occur when $p_1 = p_3 = \frac{1}{2}$ and $p_2 = p_4 = 0$.

(*d*) The case $q_1 > 0$, $q_2 > 0$ and $q_3 = 0$ gives all $p_i \neq 0$, with $p_1 > (p_2, p_3) > p_4$. The case $q_1 > 0$, $q_2 = 0$ and $q_3 > 0$ is equivalent and gives $p_1 > (p_3, p_4) > p_2$.

(*e*) The case $q_1 > 0$ and $q_2 = q_3 > 0$ gives $p_2 = p_4$. If $q_1 < (q_2, q_3)$ we find $p_1 > p_2 = p_4 > p_3$, that is, the situation

found experimentally and predicted by Monte Carlo simulations.

In summary, cases (*a*) and (*b*), related to the representation *E*, have $p_1 + p_3 = p_2 + p_4$; case (*c*), related to the representation B_1, has $p_1 = p_3 > p_2 = p_4$; and cases (*d*) and (*e*) are mixed situations of the first three cases.

An ordering related to the parameters q_2 or q_3 produces the superstructure reflections *hkl*, with $h + k = 2n + 1$, which implies doubling of the unit-cell volume with respect to the RT cell. An order driven by q_1 does not produce these kinds of superstructure reflections, because the spatial periodicity of the disordered phase is conserved. Instead, it destroys the glide plane, *n*, of the RT space group $P4/nmm$, allowing some reflections that can be indexed as *hk*0 with $h,k = 2n + 1$ in the LT unit cell. Some of these reflections have been observed for the single crystal at 150 K, but they are very weak (the most intense are 310 and $3\bar{1}0$ with $\langle I/\sigma \rangle = 8.1$) and difficult to measure *via* powder diffraction.

For the title compound, Fig. 8 shows the strain $(b - a)/a$ in the LT phase and the intensity of the strongest superstructure reflections as functions of temperature. The strain increases gradually from the transition temperature down to 30 K in an approximately linear way. Considering the 231 and 210 reflections, it is evident that at 125 K the superstructure lines are near their maximum intensities, whereas the strain is only ~50% of the maximum. The order parameters could produce several phase transitions between the different kinds of order, but the coupling of these parameters can be strong enough to make them simultaneously different from zero. Indeed, the Monte Carlo simulation predicts only one transition. The thermal evolution of the order parameters is not the same, but the parameter that collapses (*i.e.* the quadratic term in the Landau expansion becomes negative) at higher temperature grows faster when the sample is cooled below the transition temperature. From energy considerations, this parameter should be $q_2 = q_3$, as is actually observed.

Accordingly, the system undergoes the transition to an orthorhombic phase (but with *a* very close to *b*), $Z = 4$, close to the tetragonal $P\bar{4}2_1m$ group. On cooling, population p_1 gradually grows at the expense of the remaining occupancies, but p_3, which is less energetically favourable, drops faster than p_2 or p_4, that is, according to the *E* representation, which does not produce any orthorhombic distortion but produces superstructure reflections that imply a doubling of the unit cell with respect to the disordered phase. The most intense reflections in a calculated pattern for this simplified model are 230, 231, 210 and 141, which are actually observed at all temperatures below T_c in the experimental patterns (Fig. 7). Thus, the single-crystal experiment at 150 K does not 'feel' the orthorhombic distortion because it is still rather small and because of the crystal twinning. Indeed, at such a temperature, the splitting of the 040 and 400 reflections (the largest of the measured reflections) is barely resolved by powder diffraction (Fig. 7), where the experimental FWHM is about 0.2° for single reflections. The coupling between the order parameters and the lattice is driven by short-range forces, thus causing the movement of other atoms and the gradual rotation of the equilibrium orientation of the ClO_4 group, below T_c, that makes atom O3 depart from the plane containing the N atoms. All these effects produce anomalies in the thermal evolution of the superstructure reflections. The increase of the intensity of the 230 reflection, which almost doubles as the temperature falls from 120 to 30 K, is due to this rotation. Eventually, for a 15° rotation, the structure would reach *Pbma* symmetry, in a new phase transition, which has not been observed in the experimental heat capacity (Burriel *et al.*, 2002).

In $[(CH_3)_4N](BF_4)$, the orthorhombic distortion has not been observed, even in measurements made with a Guinier camera, perhaps because of the slightly smaller size of the BF_4^- ion. The repulsive short-range $BF_4 - (CH_3)_4N$ interaction could be weaker and probably the repulsive interactions among the tetramethylammonium ions play a more important role by making all the nearest-neighbour distances equal and stabilizing the tetragonal structure. The low-temperature phase could actually be orthorhombic. The fact that such a distortion is not observed could, in this case, be due to the transition temperature being lower (158 K) and the experiments being carried out only above 100 K.

This work is dedicated to Professor Domingo González, University of Zaragoza, on the occasion of his retirement. Financial support from the Ministerio de Ciencia y Tecnología and FEDER (project No. MAT2001-3507-C02-02) is acknowledged.

References

Burriel, R., Palacios, E., Melero, J. J. & Ferloni, P. (2002). *Ferroelectrics*, **270**, 393–398.
Giuseppetti, G., Mazzi, F., Tadini, C., Ferloni, P. & Torre, S. (1992). *Z. Kristallogr.* **202**, 81–88.
Ilyukhin, A. B. & Malyarik, M. A. (1995). *Cryst. Rep.* **40**, 704–705.
McCullough, J. D. (1964). *Acta Cryst.* **17**, 1067–1070.
Mylrajan, M. & Srinivasan, T. K. K. (1991). *J. Raman Spectrosc.* **22**, 53–55.
Palacios, E., Melero, J. J., Burriel, R. & Ferloni, P. (1996). *Phys. Rev. B*, **54**, 9099–9108.
Rigaku Corporation (1992). *IUSA*. Version 2.8. Rigaku Corporation, Tokyo, Japan.
Rodríguez-Carvajal, J. L., Anne, M. & Pannetier, J. (1987). *FULLPROF.* Version 3.5, updated 1997. Report 87 R014T. ILL, Grenoble, France.
Sheldrick, G. M. (1997). *SHELXL*97. Release 97-2. University of Göttingen, Germany.
Siemens (1990). *XSCANS.* Siemens Analytical X-ray Instruments Inc., Madison, Wisconsin, USA.
Subías, G., Palacios, E., Blasco, J. & García-Ruiz, J. (1996). *J. Phys. Condens. Matter*, **8**, 8971–8982.
Tolédano, J. C. & Tolédano, P. (1987). In *The Landau Theory of Phase Transitions.* Singapore: World Scientific.
Vogt, K. & Prandl, W. (1983). *J. Phys. C*, **16**, 4753–4768.